Preprint of:
Karl Bertling, John R. Tucker, Aleksandar D. Rakić "Optimum Injection Current Waveform for a Laser Range Finder Based on the Self-Mixing Effect"
Proc. SPIE 5277, 334-345 (2004)

Optimum injection current waveform for a laser range finder based on the self-mixing effect

K. Bertling, J. R. Tucker, A. D. Rakic
School of Information Technology and Electrical Engineering
The University of Queensland, St. Lucia, QLD, 4072

ABSTRACT

In a self-mixing type laser range finder the current of the laser is modulated with a triangle wave to produce a range of optical frequencies. However, the electrical signal does not produce a perfect linear sweep in optical frequency due to thermal and other effects in the laser. This leads to errors in the accuracy and resolution of the range finder. In this paper, we describe and implement a method in software to systematically determine the optimal shape of the injected waveform needed to eliminate these thermally induced measurement errors. With this method we do not require the more complicated and expensive optical techniques used by other researchers to recover the optical frequency variations with regard to injection current. The averaging of a reasonable number of samples gave sub-millimeter accuracy when the optimal current shape was used. The uncertainty in the average measurements are improved by roughly six times compared to the conventional triangular modulation. The reshaping also results in the range finding system being less sensitive to changes in ambient temperature.

Keywords: Self mixing, laser range finder, current reshaping, thermal effects, optical feedback, distance measurement

1. INTRODUCTION

External optical feedback in semiconductor lasers has been studied by many researchers [1], [2], [3]. In most cases this feedback is undesirable [4] as it can change the response and increase the intensity noise of the laser. However, this feedback has also been used for many constructive purposes such as modal analysis and defect detection [5], line width reduction [6], target displacements, range finding and velocity measurement [7], 3-D imaging [8], [9], optical microscopes [10] and various medical applications [11], [12].

The optical feedback is a result of the laser beam being partially reflected from an object back into the laser cavity. The reflected light mixes with the light inside the laser cavity and produces variations to the operating frequency of the laser. These variations can be monitored by power fluctuations in a photodiode and the resulting response can then be analysed to obtain the target distance. Processing methods utilizing either the time or frequency domains can be used to determine the distance to the target [7], [13], [14].

If the optical frequency of a laser is modulated by a triangle wave then the power variations caused by the backscattered light can be processed to produce a waveform with evenly spaced peaks. The distance to the target is proportional to the average time between these peaks.

In practice the emission frequency of the laser is assumed to be proportional to the level of current injected into the laser. However, this assumption is not entirely correct and when the current of the laser in the range finding system is modulated by a triangle wave then the peaks in the desired waveform can become unevenly spaced. This effect can lead to measurement errors with non-uniform peak spacing in the time domain and double peaks in the frequency domain. Other researchers [15], [4] have attributed this behaviour to thermal effects in the laser and show that the performance of the range finder can be improved by reshaping the injection current to produce a waveform with evenly spaced peaks.

In this paper we use an alternative method to determine the optimal shape of the injected waveform needed to remove these thermally stimulated measurement errors. This shape is systematically determined by analyzing the response of different current waveforms with the range finder in software. This eliminates the need of additional expensive

equipment and complicated experimental setups used by other researchers. We show that this method provides a low cost alternative to improving the performance of a self-mixing type range finder.

2. SELF-MIXING

The self-mixing effect occurs when the light emitted from a laser hits an object and is reflected back into the cavity of the laser. This setup can be represented using the classic three mirror Fabry-Perot cavity model [4], [7], [8], [9], [16] as shown in Fig. 1. The two mirrors of the laser cavity are represented by M_1 and M_2 with their corresponding reflection coefficients Γ_1 and Γ_{2s}. The target can also be modeled as an external mirror with a reflection coefficient Γ_{2ext}. An internal monitor photodiode integrated into the packaging of a commercial laser diode can be used to observe the changes in the optical power from the laser with self-mixing.

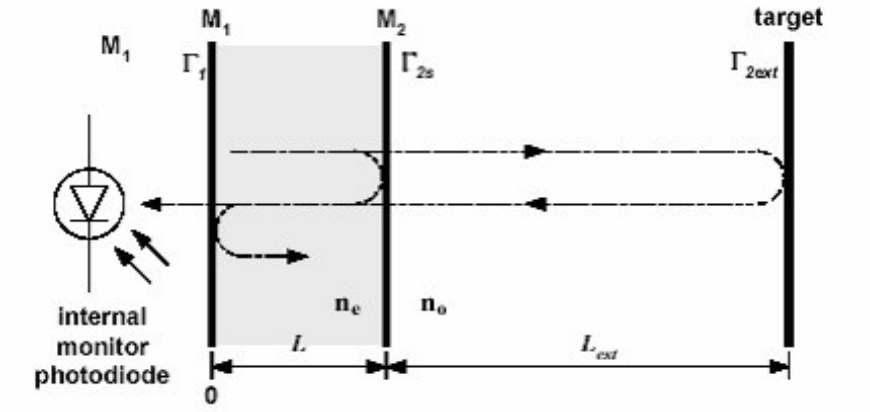

Figure 1: Three-mirror Fabry-Perot cavity model of a semiconductor laser diode

To simplify Fig. 1, the second mirror and the target can be combined into a single mirror that has a complex reflection coefficient Γ_{eff} as shown in Fig. 2 [4], [7], [8], [16].

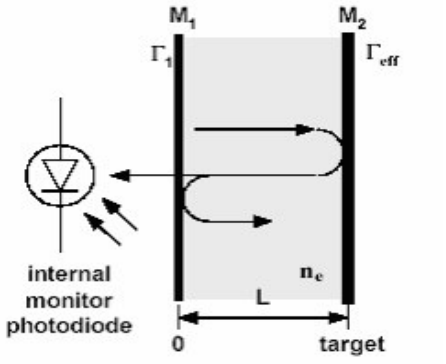

Figure 2: Equivalent Fabry Perot cavity with combined external mirror

The reflectance of this mirror changes with distance as it is proportional to the round-trip propagation time of the external cavity, τ_{ext}, and the value of reflectance is given by,

$$\Gamma_2(\upsilon) = \Gamma_{2s} + \left(1 - |\Gamma_{2s}|^2\right)\Gamma_{2ext} \exp(-j2\pi\upsilon\tau_{ext}) \qquad (1)$$

where,

υ emission frequency of laser

$\tau_{ext} = \frac{2L_{ext}}{c}$ round trip propagation time in external cavity

The light emitted from the laser has a controllable frequency and phase so the reflected light will add constructively or destructively with the light inside the laser cavity. The phase shift introduced by the round trip travel to and from the target effectively causes a phase change in the reflectivity of the mirror as indicated in equation (1). This will result in changes to the properties of the light emitted from the laser including the output frequency, the line width, the threshold gain and the output power.

In a Fabry-Perot resonator the round-trip phase shift has to be zero or an integral number of 2π for the lasing condition to be satisfied. Given this condition and setting the excess phase to zero it is possible to numerically solve for the emission frequency with feedback. Under weak feedback levels there is only one solution for the emission frequency. Solving for the emission frequency shows that there is an abrupt change at every $\lambda_{th}/2$ of target displacement, where λ_{th} is the emission wavelength without feedback, corresponding to a full 2π phase shift of the round trip.

In practice, the output of the laser can be measured in terms of its optical output power through the internal monitor laser photodiode. The laser output power is related to the emission frequency with feedback and can be written as [9],

$$P = \eta\left(I_{op} + \frac{\kappa_{ext} qV}{LT_s a\Gamma}\cos\left(2\pi\upsilon\tau_{ext}\right) - I_{th} \right) \qquad (2)$$

where,

κ_{ext} coupling coefficient of the external cavity, indicative of the quantity of light being coupled outside of the laser cavity;
q elementary charge of the electron;
V active volume of the laser cavity;
T_s spontaneous recombination rate;
a proportionality constant used in the linearised dependence of the threshold gain, g_{th}, as a function of carrier density, n, in the laser diode depending on the threshold gain carrier density characteristics;
Γ mode confinement factor;
L length of laser diode cavity;
I_{op} operating current of the laser diode;
I_{th} laser diode threshold current without feedback.

3. RANGE FINDING

Equation (2) shows that the power of the laser exhibits a sinusoidal relationship with the target distance, L_{ext}, since the round-trip propagation time of the external cavity, τ_{ext}, is proportional to the length of the external cavity. Periodic changes in the power, which also correspond to mode hops in the laser, occur at the frequency $\upsilon\tau_{ext}$ for every $\lambda_{th}/2$ of the target displacement along with a 2π phase shift of the round trip.

Since the distance to the target is the quantity to be determined, it is impractical to move the target or laser to observe the mode hops. Instead, the same observations can be made by modulating the frequency of the laser. The frequency of the light is changed so that a number of distinct resonant modes develop in the cavity with the frequency of the laser being forced to the closest one of these modes. The frequency of each mode depends on the round trip phase shift of the external cavity. Therefore, the frequency spacing between these modes is proportional to the target distance.

The change in the frequency of the light can be obtained by modulating the current of the laser with a triangle wave. The emission frequency of the laser without feedback also changes with current. Therefore, we need to introduce an additional parameter to indicate the amount by which the optical frequency changes with the injected current. This parameter is known as the frequency modulation coefficient, Ω, and is expressed in GHz/mA. We can then use this parameter to solve for the emission frequency and hence the output power.

The resulting power waveform of the laser is a triangle wave superimposed with small variations corresponding to the power fluctuations of the different resonant modes occurring in the cavity. This is shown in the simulated and experimental results for the self-mixing type range finder in Fig. 3. By differentiating the power waveform we produce the series of sharp peaks shown in Fig. 3.

(a) (b)

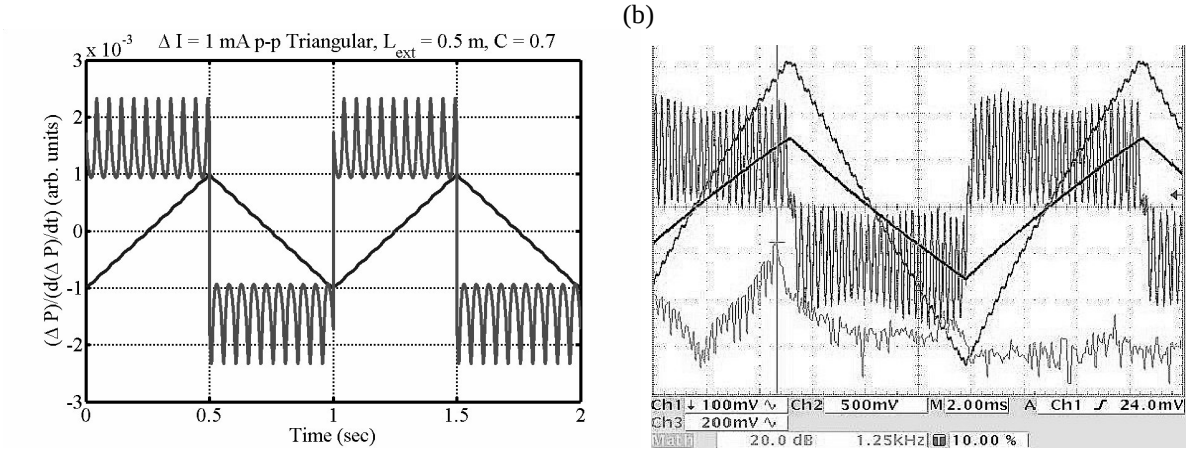

Figure 3: Simulated (a) and experimental (b) power fluctuation curves for frequency modulated laser with feedback

The peaks correspond to the resonant modes in the cavity and the frequency spacing between the modes is proportional to the average distance between the peaks. The distance to the target can then be finally calculated as [9],

$$L_{ext} = \frac{c}{8 i_{pk-pk} \Omega f_m p_{avg}} \qquad (3)$$

where,

$i_{pk\text{-}pk}$	peak to peak amplitude of the modulating current (mA)
f_m	modulating frequency
p_{avg}	average spacing between peaks (seconds)

The spacing between the peaks can be deduced by counting the number of peaks in the differentiated waveform. The normal method used by other researchers [7], [13] is to set a threshold level at which the number of peaks over this level can be counted. This number is then divided by the time between the first and last peak to give the average spacing.

There are a number of problems that arise when using this method. As the distance to the target increases there is variation in the height of the peaks and more noise. The differentiated waveform becomes more like a square wave with little peaks on the top. There is also a slope instead of a flat square wave. This is partially due to transient responses and partly due to thermal effects. There comes a point where the peaks become so small that it is impossible to a set single threshold to capture all the peaks.

To counter this problem another peak spacing method can be used where a few peaks are discarded from the beginning and end of the cycle. Although this method reduces the error obtained with the first peak spacing method it still suffers from the inherent limitations of setting a perfect threshold in the presence of noise and a low quality response.

An alternative method of acquiring the average peak spacing has been described by other researchers in previous papers [13], [14]. This method detects the average frequency of the peak occurrence in the frequency domain. The Fast Fourier Transform (FFT) of the differentiated waveform gives the frequency spectrum of the signal. Neglecting the peak due to the modulation frequency of the laser the strongest peak in the spectrum corresponds to the frequency of the peaks in the differentiated waveform. In this method there is no need to set a threshold so signals with peaks of various heights can be used. This makes the FFT method more robust than the peak spacing methods for low signal levels and in the presence of noise.

4. THERMAL EFFECTS

In the theory presented above a linear injection current should produce a linear change in the optical frequency. However, in practice this relationship is not entirely correct and at points where the current modulation changes trend large discrepancies appear. Other researchers [15], [4] have attributed this behaviour to thermal effects which are compounded at lower modulation frequencies.

These thermal effects are a result of the heat being built up in the laser cavity. The heat causes changes to various properties of the cavity so that the frequency of light is changed. These property changes include the cavity length, the index of refraction of the cavity and in the case of VCSELs a change in the mirror reflectivity [17].

The effect that these changes have on the range finding system can be observed in both the peak spacing and FFT methods. In the peak spacing methods the thermal effects cause the peaks to become unevenly spaced. In the frequency domain this translates to the spectral width of the peak frequency becoming broader since there is more variation in the time between the peaks.

This behaviour leads to errors in the precision and accuracy of the range finding system. The errors can be reduced by reshaping the injection current so that the spacing between the peaks is constant [18], [15], [4].

The shape of the desired waveform can be obtained by measuring the phase shift and amplitude loss of the optical frequency variations over the injection current variations as described by Gouaux et al. [15]. This procedure uses a complicated experimental setup and a complex analysis to obtain the modified waveform.

A recent method used by Bosch et al [19] to reduce the resolution and error of the range finding system is to use a Mach Zehnder interferometer. This setup eliminates the extra chirp created by temperature and other effects and leads to constant spacing between the peaks.

However, both these methods require additional and involved optical experimental setups to make the spacing between the peaks constant. In this paper we propose a new method to obtain the desired waveform by using only the range finder itself. This method uses a wide range of synthesized current waveforms to systematically determine the optimal shape of the injection current. This leads to a lower cost system and less complicated setup since no extra hardware components are needed. Also, by optimizing the injection current with the range finder resolution as an objective function we are effectively taking other non-idealities of the system into account.

5. CURRENT RESHAPING

By adjusting the injection current modulation waveform the differences between the average peak spacing in the processed optical signal can be eliminated. The different average spacing manifests itself as two peaks in the FFT frequency spectrum of the differentiated optical output signal. In most cases the peaks are close enough to be seen as a single wide peak. However, once the resolution of the spectrum is increased or thermal effects are intentionally introduced then the separation of the two peaks becomes more obvious as shown in Fig. 4.

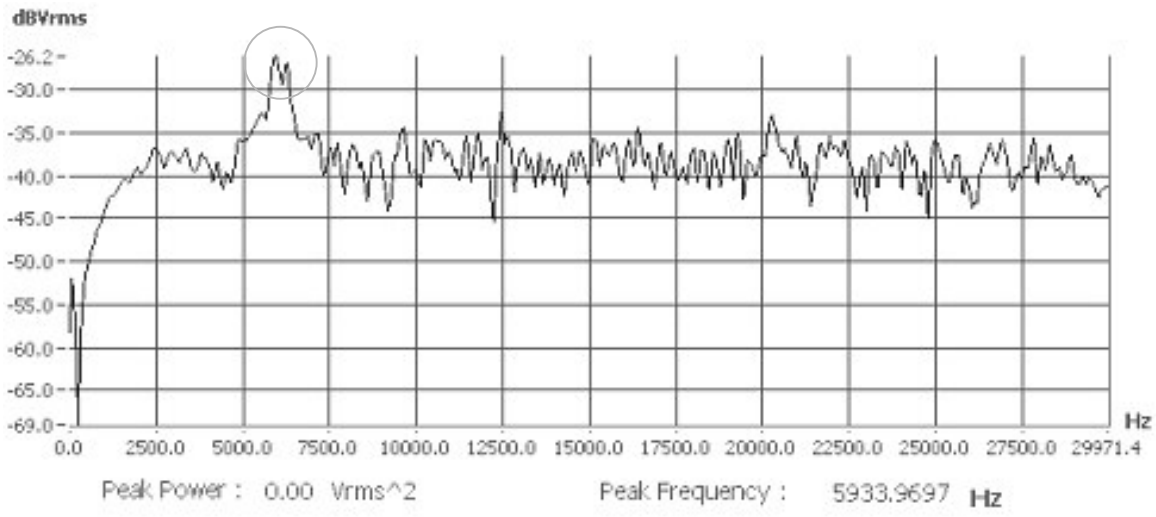

Figure 4: Dual peaks observed due to thermal effects

By inspecting the time domain signal of the peaks, other researchers [15], [4] have noted that the spacing between the peaks in the upward transitions is less than those in the downward transition with more peaks occurring in the upward transition then the downward transition. In the frequency domain this means that the average peak spacing in the upward slope transition has a lower peak frequency in the FFT spectrum. This indicates that the more dominant of the two peaks in Fig. 4 is that of the upward slope.

With this knowledge, only the downward current modulation slope was reshaped. The intended effect of the reshaping is to reduce the spectral width of the FFT spectrum or to shift the center frequency of the downward slope peak to be the same as that of the upward slope peak. A simplified comparison between the expected results of reshaping on the FFT spectrum compared to the standard triangle wave modulation is shown in Fig. 5.

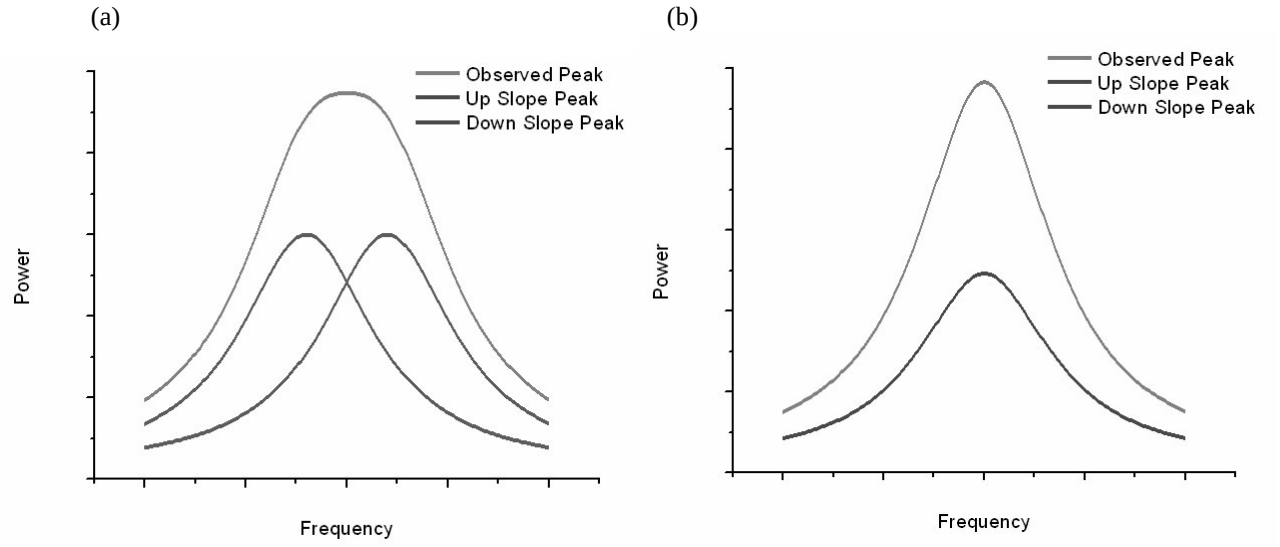

Figure 5: (a) Simplified Effect of Triangle Wave Modulation (b) Simplified Effect of Reshaped Modulation

The form of the reshaping was built around the idea that the laser cavity should dissipate some of the heat built up during the upward slope. This can be achieved with a sharp exponential drop at the start of the downward modulation onto a linear line. The linear line is needed so that the heat is dissipated at the same rate as it is generated in the upward slope. This leads to the following equation:

$$f(x) = \varepsilon e^{-\alpha x} + \beta x + \gamma \qquad (4)$$

Now by constraining the equation to pass through the starting and finishing positions of the previous triangular down slope the number of variables can be reduced through the following substitution:

$$\varepsilon = 1 - \gamma \qquad (5)$$

$$\beta = \varepsilon e^{-\alpha} - \gamma \qquad (6)$$

Ultimately this makes γ control the intercept of the linear line and α control the exponential drop to the line. In Fig. 6 the difference between the reshaped (4) and original down slope modulation can be seen as well as the contributing factors of each of the components of *f*(*x*).

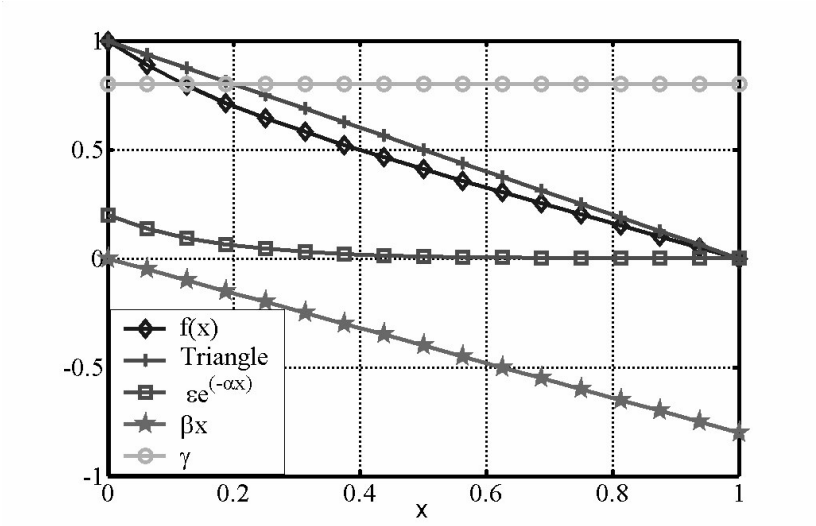

Figure 6: An example of *f(x)*, compared to original triangle slope, and its individual components

Using this function and sweeping through various values of α and γ a data set containing a number of different curves can be created. This data set can then be used by software to subsequently cycle through each different curve with the range finder. The performance of the range finder with each curve can be recorded in software so the optimal injection waveform can be determined.

6. EXPERIMENTAL SETUP

For this experiment, an Emcore VCSEL (Gigalase 8585-8312) that emits a single longitudinal mode of light with an internal monitoring photodiode was used. The laser has a threshold current of 1.5 mA and a typical peak wavelength of 850 nm.

The block diagram for the implemented ranging system is shown in Fig. 7. The desired modulation waveform is sent from the PC using the LabView software package to the arbitrary waveform generator (Agilent 33220A). The generator is then instructed by LabView to produce the waveform with a 300 mV peak-to-peak voltage and at a frequency of 75 Hz. This voltage is then converted into a current by the laser driver circuit to modulate the laser with a corresponding

current fluctuation of 0.32 mA peak to peak. The laser driver circuit also sets the DC bias current of the laser above threshold at 4 mA.

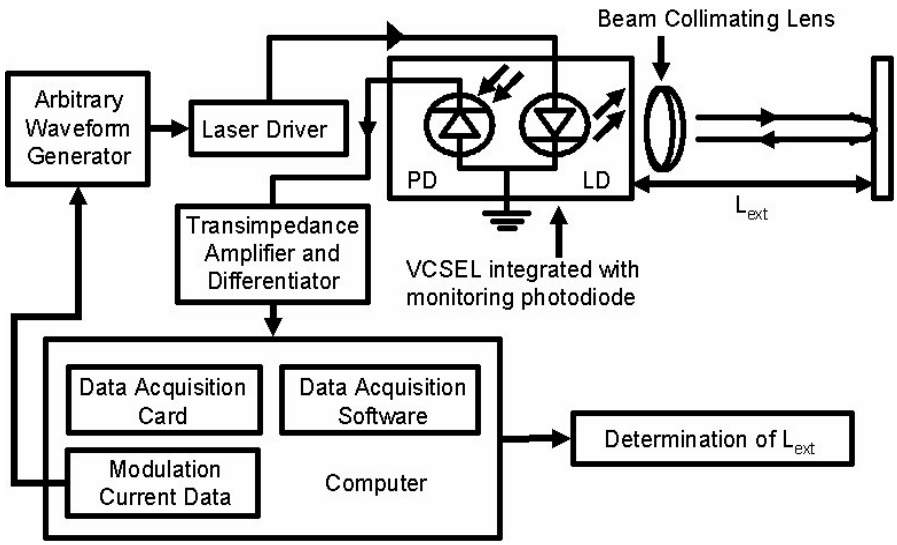

Figure 7: Block Diagram of Experimental Setup

The VCSEL is placed in a mount, which is fixed on an optical rail. The laser beam output from its rear mirror is monitored by the photodiode. A lens is used to collimate the laser beam. The target is made from a circular piece of sandblasted aluminum mounted on an adjustable X-Y-Z platform. This material is chosen because it behaves like a diffuse reflector.

The light from the laser is reflected from the target back into the laser cavity where the internal monitor photodiode is used to detect the power fluctuations in the light. These fluctuations can be detected since the current that flows through the photodiode is proportional to the power of the light emitted from the laser. The photocurrent is then converted to a voltage with the transimpedance amplifier and sent to the differentiator circuit. The output of the differentiator produces a waveform with sharp peaks and is connected to a National Instruments 12-bit data acquisition card in the PC.

LabView was then used to perform additional signal processing on the differentiated power signal to improve the accuracy and stability of the range finding system. An inverse Chebyshev 2nd order high pass filter was first applied to the differentiated signal in LabView to ensure that peak frequency detected with the FFT method was not the strong 75 Hz frequency component of the current modulating wave. Subsequently, a 7-term Blackmann-Harris window was used to smooth the signal in the frequency domain. Additional averaging was also was also performed, for some of the measurements, over a number of periods to obtain better accuracy.

Each injection current waveform was cycled through taking 60 samples for each different curve and saving the FFT spectra to disk. The spectra were then analyzed in Matlab by averaging the 60 samples and fitting Gaussian peaks to the area of where the peak frequencies existed.

7. RESULTS AND ANALYSIS

Two factors were considered when finding the optimal point from the α and γ sweep. The first was the difference between the center frequencies of the two major peaks from the upward and downward slopes of the current modulation and the second was the peak power of the FFT spectrum. During preliminary sweeps it was found that good results were occurring with values of α ranging from 0.2 to 2.0 and γ from 0.75 to 0.95 in the ambient temperature range 22.0 to 24.0 °C.

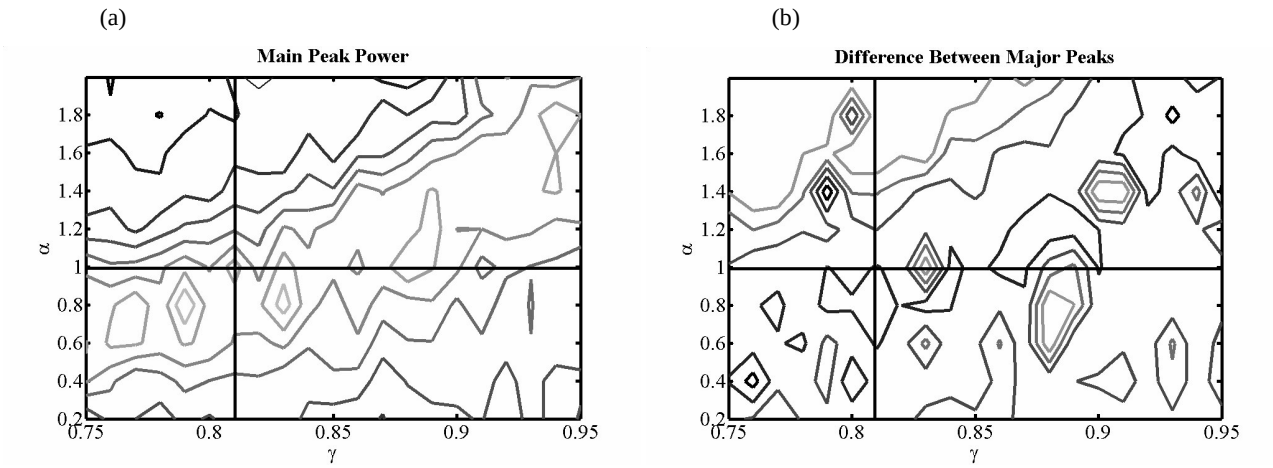

Figure 9: Sweep of α & γ at 22.3 to 22.4 °C (a) Main Peak Power, (b) Major Peak Difference.

Figure 9 (a) shows the main peak power as a function of parameters α and γ. The lighter contours on the edge of the contour plot correspond to greater peak powers. From this we can see that there are a set of near-optimal points along a diagonal line of a contour plot. Similar conclusions can be drawn from Fig 9 (b) showing the difference between the two prominent peaks in FFT spectrum as a function of α and γ parameters. Again, the area of the plot in the vicinity of the diagonal provides minimum separation between the two peaks and consequently improved resolution of the range finder.

To observe more closely the effect of the upward and downward peaks on the optimal point the power of different frequencies in the FFT spectrum are recorded. This is shown in Fig. 10 for a range of values of α and γ that lie along a diagonal line of points passing through the cross hairs shown in Fig. 9. As can be observed, the downward peak starts at a higher frequency, and as α and γ increase it is shifted towards lower frequencies. It is worth noting that shape of the FFT spectrum at α = 0.2 is nearly identical to what is observed with the triangular current waveform, while α = 0 reduces the current waveform to the triangle waveform.

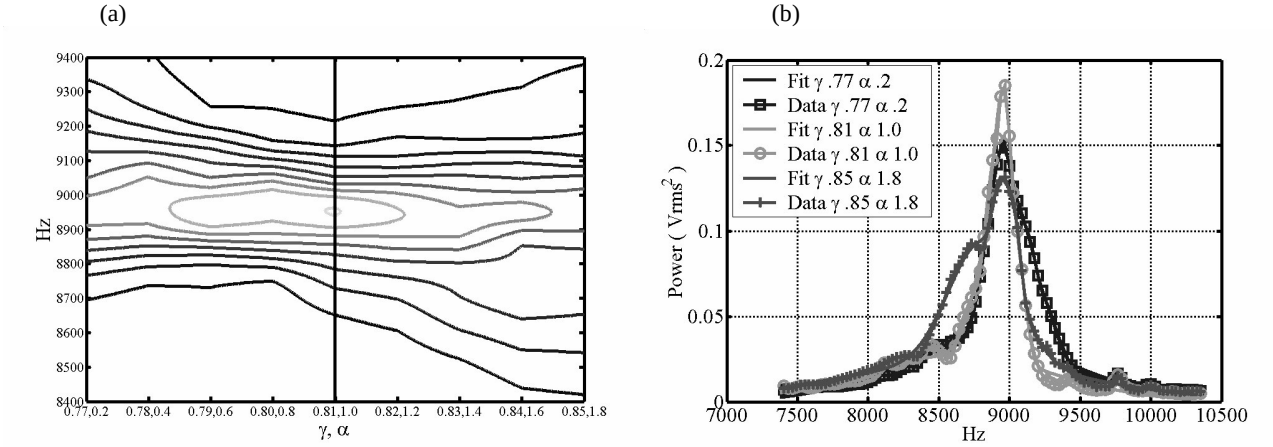

Figure 10: Sweeping of α & γ diagonally across the optimal point at 22.3 to 22.4 °C (a) Increasing α & γ vs. FFT Spectra Frequency, (b) Data & Fits showing various cross-sections from (a).

Figure 11 shows the improvement of the FFT spectrum as seen in LabView with the use of the reshaped injection current waveform determined from the optimal point, at a target at length 0.3 m. The reshaped current waveform has a higher peak power, a smaller spectral width and less noise than the triangle wave modulation scheme.

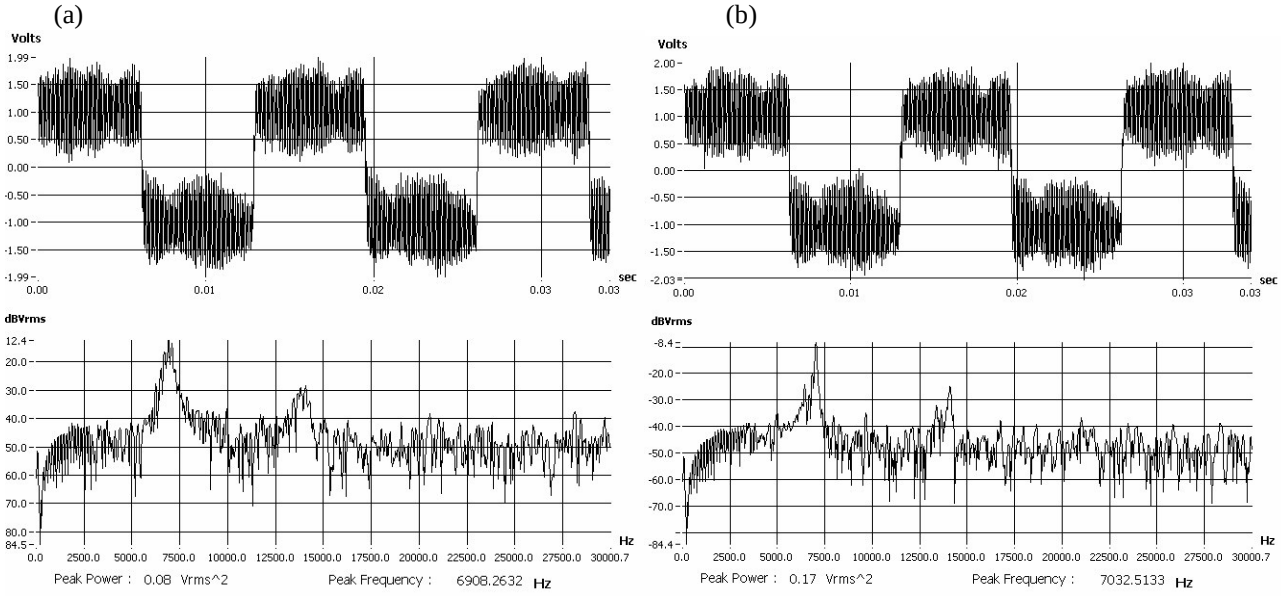

Figure 11: (a) Typical Triangle Differentiated optical output & FFT Spectrum. (b) Typical Reshaped Differentiated optical output & FFT Spectrum.

This improvement corresponds to an increase in the accuracy and reduction of the uncertainty of the distance measured. Figure 12 shows the variation of distance and ambient temperature over time with a target at 0.4 m using the reshaped and triangle modulation schemes. These readings were taken every five minutes over 50 minutes from an average of 500 samples.

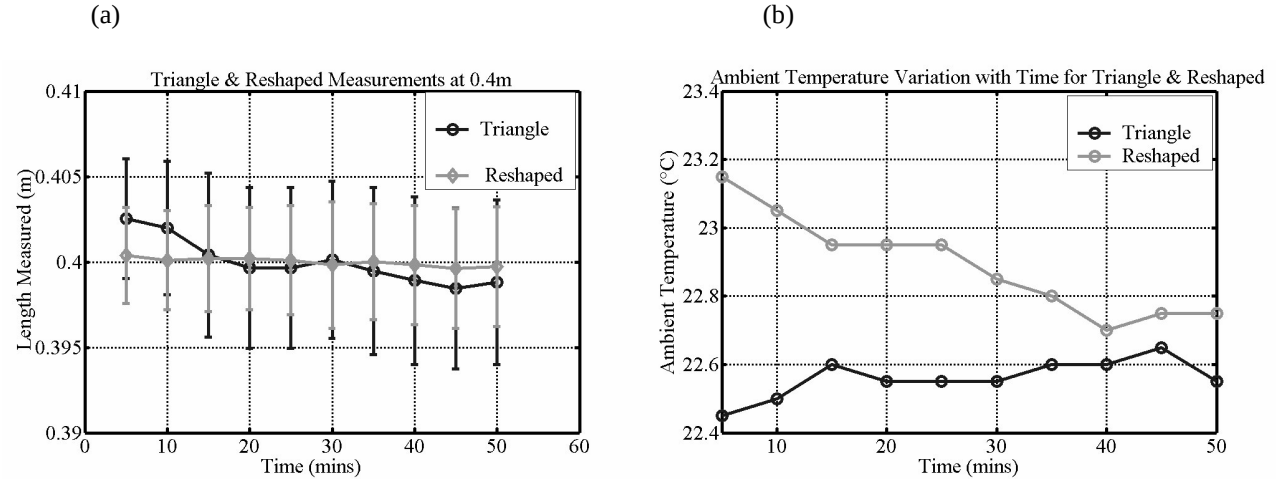

Figure 12: (a) Variation in time of measured length of Triangle and Reshaped modulation schemes. (b) Variation in time of temperature of the Triangle and Reshaped modulation schemes.

The uncertainty calculated for the 500 samples that are averaged, is taken as the standard deviation of the distribution of the sampled measurements. With the triangular modulation scheme the uncertainty is 5 mm compared to the 3 mm obtained with the reshaping. Looking at the averages of the 500 samples, there is a 1.5 mm difference over time using the triangular modulation scheme and 0.25 mm difference using the reshaped modulation. From this we can see that the reshaped current has less variation and is more accurate with a noticeable improvement from the triangle waveform.

With the triangular modulation scheme we can see that the change in measured distance over time in Fig. 12 (a) follows the change in ambient temperature over time. This effect is still present for the reshaped modulation but its effect is greatly reduced. This shows that the range finding system with reshaping is less sensitive to changes in ambient temperature and can operate over a wider range of temperatures.

The optimal injection waveform was then used to measure a wide range of distances. The results are shown in Fig. 13. These results also confirm that the reshaped waveform gives better accuracy and less variation of distance.

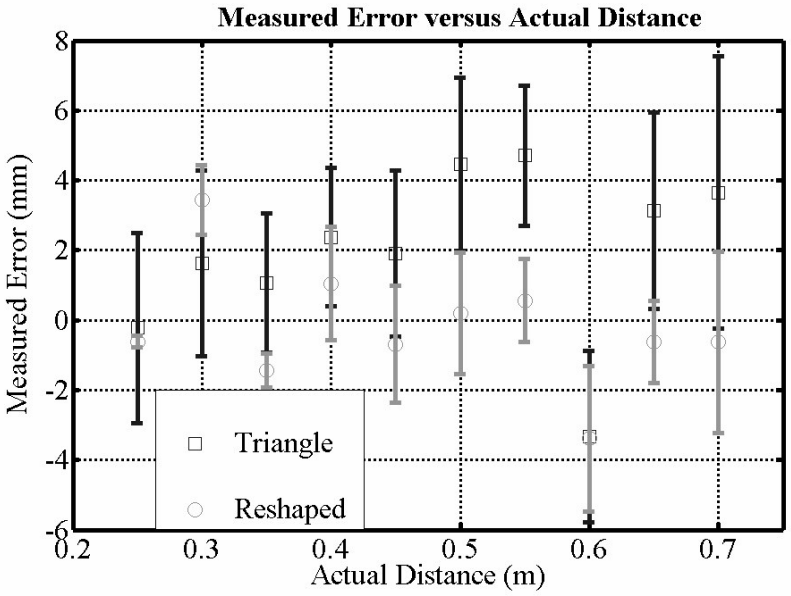

Figure 13: Measured Error of Reshaping and Triangular Current Waveforms

8. CONCLUSIONS

In this paper the accuracy and uncertainty of a self mixing type laser range finder has been improved by reshaping the modulation current to consider thermal effects. A novel method for obtaining the optimal current waveform based on the optimization procedure has been described and implemented. This method has advantages in cost and ease of implementation compared to the more complicated and expensive optical techniques other researchers have used to reshape the injection current [18], [15], [4]. With sufficient averaging sub-millimeter accuracy can be achieved when thermal effects are taken into account through current reshaping. A six-fold reduction in uncertainty in the average measurement when compared to the triangular modulation was achieved. The range finding system is also less sensitive to changes in ambient temperature with reshaping, which relaxes the requirement of extra hardware to stabilize the temperature of the laser. This is an important advantage if the device is to be used in a battery operated system.

REFERENCES

1. R. Lang, and K. Kobayshi, “External Optical Feedback Effects on Semiconductor Injection Laser Properties,” *IEEE J. Quantum Electron.*, **QE-16**, 347-355, 1980.

2. J. Helms, and K. Petermann, “A Simple Analytic Expression for the Stable Operation Range of Laser Diodes with Optical Feedback,” *IEEE J. Quantum Electron.*, **26**, 833-836, 1990.
3. K. Petermann, “External Optical Feedback Phenomena in Semiconductor Lasers,” *IEEE J. Select. Topics Quantum Electron.*, **1**, 480-489, 1995.
4. N. Servagent, G. Mourat, F. Gouaux, and T. Bosch, “Analysis of some intrinsic limitations of a laser range finder using the self-mixing interference,” *Proc. SPIE*, **3479**, 76-83, 1998.
5. N. Servagent, T. Bosch, and M. Lescure, “A Laser Displacement Sensor Using the Self-Mixing Effect for Modal Analysis and Defect Detection,” *IEEE Trans. Instrum. Meas.*, **46**, 847-850, 1997.
6. G. P. Agrawal, “Line Narrowing in a Single-Mode Injection Laser Due to External Optical Feedback,” *IEEE J. Quantum Electron.*, **QE-20**, 468-471, 1984.
7. T. Bosch, N. Servagent, F. Gouaux, and G. Mourat, “The self-mixing interference inside a laser diode: application to displacement, velocity and distance measurement,” *Proc. SPIE*, **3478**, 98-108, 1998.
8. T. Bosch, N. Servagent, R. Chellali, and M. Lescure, “Three-dimensional object construction using a self-mixing type scanning laser range finder,” *IEEE Trans. Instrum. Meas.*, **47**, 1326-1329, 1998.
9. E. Gagnon, and J. F. Rivest, “Laser range imaging using the self-mixing effect in a laser diode,” *IEEE. Trans. Instrum. Meas.*, **48**, 693-699, 1999.
10. Y. Katagiri, and S. Hara, “Scanning probe microscope using an ultrasmall coupled-cavity laser distortion sensor based on mechanical negative-feedback stabilization,” *Meas. Sci. Technol.*, **9**, 1441-1445, 1998.
11. K. Mito, H. Ikeda, M. Sumi, and S. Shinohara, “Self-mixing effect on the semiconductor laser Doppler method for blood flow measurement,” *Medical and Biological Engineering and Computing*, **31**, 308-310, 1993.
12. L. Scalise, W. Steenbergen, and F. de Mul, “Self-mixing feedback in a laser diode for intra-arterial optical blood velocimetry,” *Appl. Opt.*, **40**, 4608-4615, 2001.
13. J. R. Tucker, Y. L. Leng, and A. D. Rakic, “Laser range finding using the self-mixing effect in a vertical-cavity surface-emitting laser,” *Conference on Optoelectronic and Microelectronic Materials and Devices*, 583-583, IEEE, Sydney, Australia, 2002.
14. M. Wang, “Fourier transform method for self-mixing interference signal analysis,” *Optics & Laser Technology*, **33**, 409-416, 2001.
15. F. Gouaux, N. Servagent, and T. Bosch, “Influence of the Thermal Effects on the Accuracy of a Backscatter-Modulated Laser Diode Range Finder,” *3rd International Congress on Optoelectronics, Optical Sensor and Measuring Techniques*, Erfurt, Germany, 1998.
16. F. Gouaux, N. Servagent, and T. Bosch, “Absolute distance measurement with an optical feedback interferometer,” *Appl. Opt.*, **37**, 6684-6689, 1998.
17. J. Dudley, D. Crawford, and J. Bowers, “Temperature dependence of the Properties of DBR Mirrors Used in Surface Normal Optoelectronic Devices,” *IEEE Photo, Tech. Lett.*, **4**, 311-314, 1992.
18. S. Shinohara, H. Yoshida, H. Ikeda, K. Nishide, and M. Sumi, “Compact and High Precision Range Finder with Wide Dynamic Range and Its Application,” *IEEE Trans. Instrum. Meas.*, **41**, 40-44, 1992.
19. T. Bosch, S. Pavageau, D. D’Alessandro, N. Servagent, V. Annovazi-Lodi, and S. Donati, “A low cost, optical feedback range-finder with chirp control,” *18th IEEE Instrumentation and Measurement Technology Conference*, IEEE, 2, 1070-1074, Budapest, Hungary, 2001.